JRC Technical Notes

IMAGE-2006 Mosaic: Geometric and Radiometric Consistency of Input Imagery

v.1.0

Pierre Soille and Jacopo Grazzini

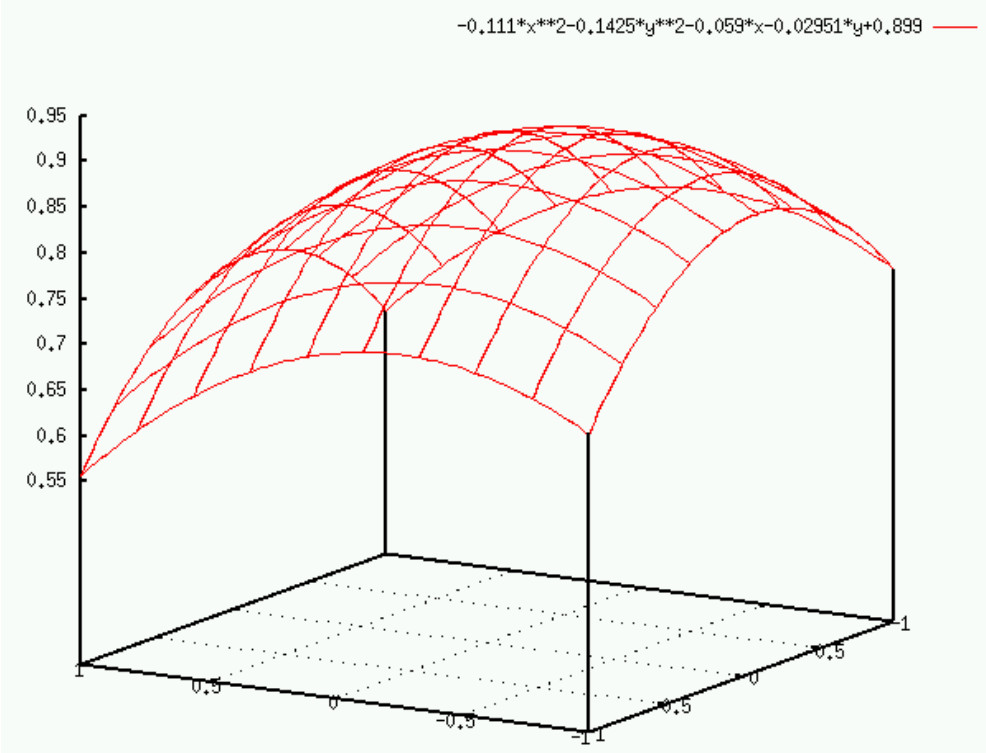

EUR 23636 EN

JRC EUROPEAN COMMISSION

ies Institute for Environment and Sustainability

The mission of the Institute for Environment and Sustainability is to provide scientific-technical support to the European Union's Policies for the protection and sustainable development of the European and global environment.

European Commission
Joint Research Centre
Institute for Environment and Sustainability
Spatial Data Infrastructures Unit

Contact information
Address: via E. Fermi 2749, I-21027 Ispra (Italy)
E-mail: Pierre.Soille@jrc.ec.europa.eu
Tel.: int+39-0332 785 068
Fax: int+39-0332 786 325

http://ies.jrc.ec.europa.eu/
http://www.jrc.ec.europa.eu/

JRC 49168

EUR 23636 EN
ISBN 978-92-79-20959-8
ISSN 1831-9424
doi:10.2788/50967

Luxembourg: Publications Office of the European Union, 2011

IMAGE-2006 Mosaic: Geometric and Radiometric Consistency of Input Imagery —v.1.0—

Pierre Soille and Jacopo Grazzini
COSIN Action
IES-Spatial Data Infrastructures Unit

December 5, 2008

Abstract

Within their domain of overlap, two images may differ in both geometry and radiometry. Consequently, when they are mosaiced, these differences may reveal the position of the seam lines even if they follow salient image structures such as roads and streams. A pair of overlapping images is said to be consistent if they are in agreement to one another in both geometry and radiometry. In this report, the consistency is measured using correlation computations and linear regressions. Measurements are produced for all existing pairs of overlapping images (given the 3,699 IMAGE-2006 input images, there are 29,447 such pairs). The quality layers of the IMAGE-2006 mosaics rely directly on these measurements. Indeed, the agreement between any pair of adjacent pieces of the mosaic is determined by the consistency measurements calculated within the domain of overlap of the two images leading to these two mosaic pieces.

Contents

1 Introduction

Within their domain of overlap, two images may differ in both geometry and radiometry. Consequently, when they are mosaiced, these differences may reveal the position of the seam line even if they follow salient image structures such as roads, streams, or field boundaries. A pair of overlapping images is said to be *consistent* if they are in agreement to one another in both geometry and radiometry. Geometric consistency measurements are derived from normalised cross-correlation computations in the spatial domain. Radiometric consistency measurements are derived by estimating the correlation coefficients and parameters of the linear regressions mapping the reflectance values of an image to those of its overlapping image.

The input 3,699 IMAGE-2006 images lead to 29,447 pairs of overlapping images when considering data region of interest (DROIs). This number decreases to 26,119 when considering country based regions of interest (CROIs). The number of overlapping pairs between all possible sensor combinations is given in table 1.

Table 1: Number of between sensor overlapping pairs based on DROIs (left) and CROIs (right). Overlapping pairs where the search for control points lead to less than 7 points have been discarded.

	SP4	SP5	IL3
SP4	3608	2668	7888
SP5	2668	1296	4812
IL3	7888	4812	6996

	SP4	SP5	IL3
SP4	3232	2366	6460
SP5	2366	1176	3942
IL3	6460	3942	5923

Contrary to consistency measurements, *accuracy* measurements require comparisons with a reference data set that can be considered as the ground truth. Geometric accuracy with respect to the reference used for orthorectification (IMAGE-2000 [6] and USGS Land Cover reference [11] datasets, the latter for all countries that were not participating to IMAGE-2000) is detailed elsewhere [5].

This report is organised as follows. The methods used for assessing the geometric and radiometric consistency are described in Secs. 2 and 3 respectively. The type of stored data is detailed in Sec **??**. Summary statistics for overlapping image pairs originating from the same or different sensors as well as those from the same or different countries are presented in Sec. 5. Concluding remarks are the subject of Sec. 6.

2 Geometric consistency

Geometric consistency is determined using normalised cross-correlation [1, 4]. In mathematical terms, the normalised cross-correlation γ function between an image f and a template t is defined as follows:

$$\gamma(u,v) = \frac{\sum_{x,y}\left[f(x,y) - \overline{f}_{u,v}\right]\left[t(x-u,y-v) - \overline{t}\right]}{\sqrt{\sum_{x,y}\left[f(x,y) - \overline{f}_{u,v}\right]^2}\sqrt{\sum_{x,y}\left[t(x-u,y-v) - \overline{t}\right]^2}}, \qquad (1)$$

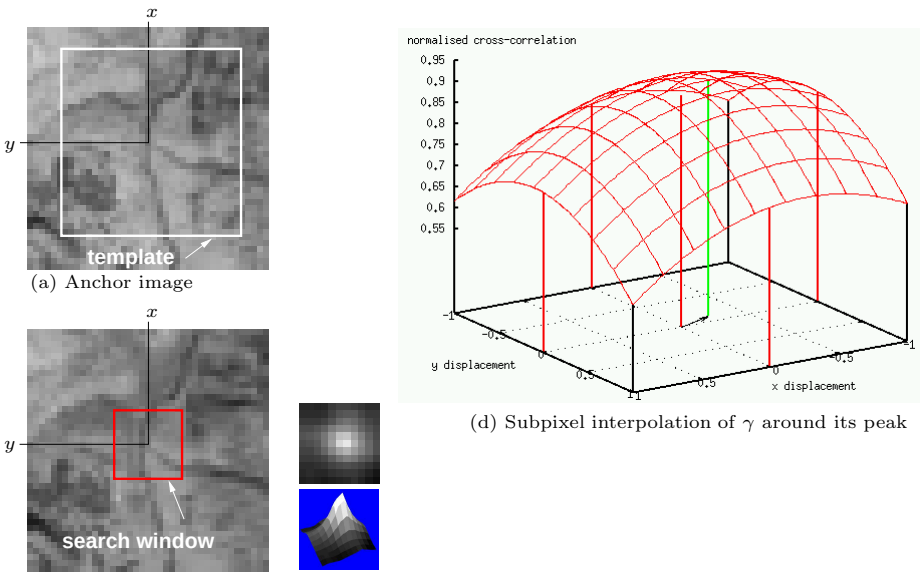

(a) Anchor image

(b) Slave image

(c) Cross correlation function γ and its 3-D representation

(d) Subpixel interpolation of γ around its peak

Figure 1: Geometric consistency assessment between an overlapping image pair: example of cross correlation calculations at a grid node of coordinates (x, y). See text for details.

where the sum is carried over the window containing the template t centred at (u, v), $\overline{f}_{u,v}$ denotes the mean value of $f(x, y)$ within the domain of the template t shifted to (u, v), and $\overline{t}$ denotes the mean value of the template. That is, $\gamma(u, v)$ gives a measure of the degree of similarity between an image and a template centred at coordinates (u, v). The measure is normalised in the sense that the observed intensity values are modified by subtracting their mean value and dividing them by their standard deviation. Consequently, the normalised cross-correlation is invariant to changes in image amplitude such as those caused by changing illumination conditions. The range of the correlation function is equal to the interval $[-1, 1]$, a value of 0 being obtained for uncorrelated windows.

In practice (see Fig. 1), given a pair of overlapping images, we arbitrarily call the first image the *anchor* image and the second the *slave* image. A template of fixed size is created by cropping the anchor image at a given position corresponding to a node of a sampling grid. The normalised cross-correlation function is computed in the spatial domain within a search window of fixed size located at the same position in the slave image. The vector separating this position from the position at which the maximum value of the normalised cross-correlation function occurs is used as a local estimation of the translation between the anchor and slave images. The subpixel position and value of the maximum is calculated by interpolating the correlation function. This interpolation is achieved by determining the paraboloid passing through the 5 points corresponding to the point maximising the discrete correlation function and its four direct neighbours, see points materialised by the five vertical red line segments in Fig. 1d. The position at which the maximum of this paraboloid occurs (see green line segment in Fig. 1d) is used as subpixel estimation of the

actual maximum of the correlation function. The maximum interpolated value corresponds to the output of the paraboloid function at this position (the upper bound being set to 1.0). This subpixel registration method is known as correlation interpolation by a quadratic estimator [10]. With this method, the accuracy of the lateral translation measurements reduces from ± 0.5 to ± 0.1 pixel (worst case). The actual accuracy depends on how well the correlation function around its peak approximates a quadratic function [2].

Only those points whose cross-correlation function lead to a clear maximum with isotropic behaviour are retained. More precisely, the following steps are considered for each pair of overlapping images:

- determine the domain of overlap between anchor and slave;
- for each node of a pan-European grid of width of 40 pixels (i.e., the coordinates of all nodes are equal to a multiple of 1000m) falling within the domain of overlap and without clouds[1], determine the position and magnitude of the maximum of the normalised cross-correlation using a template of width equal to 31 pixels and a search width in the slave image equal to 15 pixels. That is, it is expected that the maximum horizontal and vertical displacements does not exceed 7 pixels and that a template pf 31 pixels is large enough to ensure that high correlation values will only be obtained for actually matching points.
- select all points whose maximum normalised cross-correlation is greater than or equal to 0.75 and whose aspect ratio (ratio of major to minor axis) is less than or equal to 1.1;
- calculate the x and y displacements for each selected point;
- output in an ASCII file the mean, the root mean squared error (RMSE), and the standard deviation of all calculated displacements.

Given the sheer amount of image pairs to test, the computations were performed on a distributed system so that up to 24 pairs of overlapping images were processed in parallel.

3 Radiometric consistency

Radiometric consistency between all pairs of overlapping images is evaluated by comparing either the digital numbers or the top of atmosphere values of each pair of intersecting images within their domain of overlap not contaminated by clouds. This is achieved by determining the coefficients of the linear transformation mapping the values of the slave image to that of the anchor image (method sometimes called 'simple regression' [3, 12]). These coefficients are calculated for each band by performing a linear regression (one per band). In mathematical terms, denoting by x (resp. y) the top of atmosphere reflectance values (or the input digital numbers) in the anchor (resp. slave) images, the following linear transformation is estimated:

$$y^\star = ax + b.$$

[1] Clouds were detected using the method described in [7].

The coefficients of this linear transformation are determined by minimising the sum of the square of the differences between the observed and estimated values: $\sum_i (y_i^\star - y_i)$. This leads to coefficients expressed in terms of the mean μ and standard deviation σ values:

$$\begin{aligned} a &= \sigma_{XY}/\sigma_X, \\ b &= \mu_Y - a\mu_X. \end{aligned}$$

The correlation coefficient ρ_{XY} indicates the strength and direction of the calculated linear relationship between the slave and anchor intensity values:

$$\rho_{XY} = E\big[(X-\mu_X)(Y-\mu_Y)\big]/(\sigma_X\sigma_Y). \tag{2}$$

Note the similarity of this equation with the normalised cross-correlation function at the basis of the geometric consistency measurements (Eq. 1). Finally, the residual variance of the errors (referred to as err in the generated file) is also computed:

$$\text{err} = \sum_i (x_i - y_i^\star)^2/n = (1-\rho_{XY}^2)\sigma_Y^2,$$

with n equal to the number of pixels in the ROI without clouds. Perfectly matching overlapping image pairs have unitary slopes (a), zero offset (b), unitary correlation coefficients ρ_{XY}, and zero residual variance err.

4 Stored data

Output measurements for both geometric and radiometric analysis are stored in an ASCII file whose name contains the names of the anchor and slave images. An example of output measurements produced for an overlapping image pair is displayed in Fig. 2. This file highlights that the relative displacement between the two input scenes exceeds 2 pixels in the y direction and is close to 1 pixel in the x direction. The radiometric dissimilarity between the two scenes is revealed by the low correlation values obtained for all bands. The two scenes are displayed in Fig. 3 with a zoom highlighting the measured mean displacement between the scenes. Figure 4 displays the scattergram calculated for each band of the two scenes within their domain of overlap and, contrary to the method used for calculating the regression coefficients, *without* suppressing regions contaminated by clouds. The presence of haze and clouds as well as illumination conditions and phenological differences (mid June to end of July in two different years) explain the rather low correlation values.

The generated ASCII files are stord in the directories `2006_COV12-QREG-XROI` and `2006_REF-QREG-XROI` where the letter `X` equals either `D` or `C` depending on the type of ROI used for the calculations. The files are organised using the level 18 of the European reference grid.

5 Results

Geometric and radiometric consistency measurements described in the previous section were computed for all pairs of overlapping images using both DROIs and CROIs. For CROIs, the regions beyond the territory of the 38 participating

```
ANCHOR 2006_COV1/42-A/20060615-1027_SP4_IP-B4FR_4130223241-DB.tif
SLAVE  2006_COV1/42-A/20070726-1018_SP4_IP-B4FR_4083323430-AB.tif

NPIX_IN_ROI 947443
NPIX_IN_ROI_WITHOUT_CLOUDS 884756
PERCENTAGE_WITHOUT_CLOUDS 0.933836

RELATIVE GEOMETRIC CONSISTENCY:
TEMPLATE_WIDTH 31
SEARCH_WIDTH 15
GRID_WIDTH 40
PIXELS_WITH_NCC_CALCULATED 975.0
PIXELS_WITH_ABS(NCC)_GEQ_0.750000 305.0
PIXELS_WITH_ABS(NCC)_GEQ_0.750000_AND_ELLIPSIS_ASPECT_RATIO_LEQ_1.100000 293.0
X_MEAN_(m) 17.568
Y_MEAN_(m) -52.159
X_RMSE_(m) 18.834
Y_RMSE_(m) 52.204
X_STD_(m) 6.788
Y_STD_(m) 2.179

RELATIVE RADIOMETRIC CONSISTENCY:
REG_PARAM(dn) [a b corr err]
  1:  0.856  16.774  0.688  696.138
  2:  0.568  36.711  0.530  383.561
  3:  0.976  34.118  0.749  1027.421
  4:  0.675  31.181  0.729  517.678
REG_PARAM(toa) [a b corr err]
  1:  0.897  8.199  0.687  164.691
  2:  0.592  24.698  0.529  168.559
  3:  0.686  7.535  0.749  50.235
  4:  0.713  8.030  0.729  34.046
```

Figure 2: Output measurements of geometric and radiometric consistency checks. The rather high geometric and radiometric deviations between this pair of images is highlighted on Fig. 3.

countries plus a buffer of 5km (200 pixels at a resolution of 25m) have not been taken into account. A pair was deemed overlapping if at least 7 control points, in the sense of the threshold values detailed in Sec. 2, were found.

In this section, we present a series of synoptic tables digesting the information stored in the 55,566 files (29,447 for DROIs and 26,119 for CROIs). Wherever appropriate, these tables are given on a country and sensor basis. Beware that all country codes used in this report are referring to the codes used in the data delivered to JRC and therefore depart sometimes from normalised codes, see details in [8].

5.1 Geometric consistency

An evalutation of the relative correspondence between overlapping pairs sorted on a sensor basis is summarised in tables 2–4 by indicating the mean, the RMSE, and the maximum of mean x-y displacements. These tables show that the geometric consistency, when considering pairs of identical sensors, increases in the following order: SP4, IL3, and SP5, the SP5 and IL3 values being very similar.

Measurements obtained for overlapping image pairs originating from the same country are summarised in table 5 for CROIs. This table indicates the average of the mean displacements, the average of the RMSE values as well as the maximum mean displacement among all selected overlapping pairs. It shows that the average of mean x-y displacements is below half a pixel for

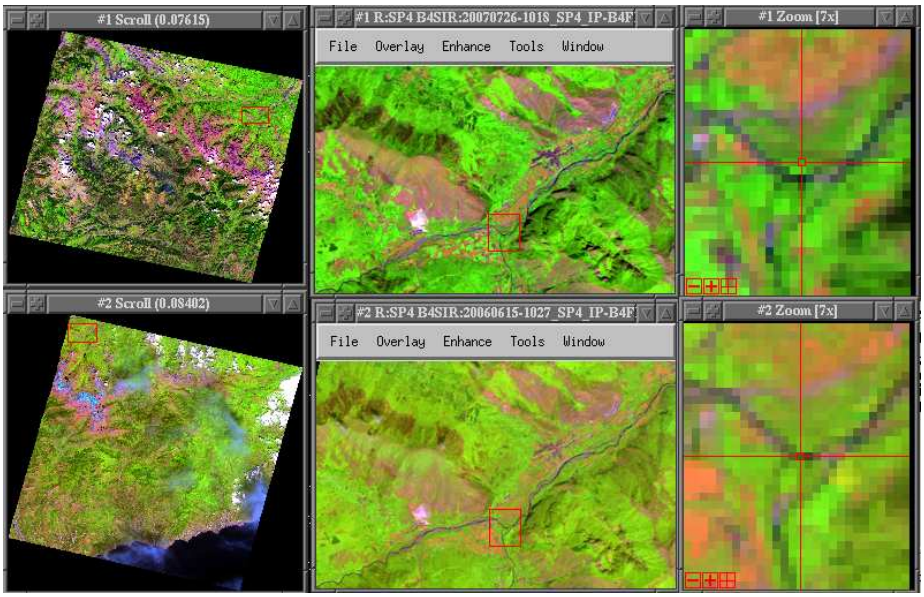

Figure 3: Example of two SPOT4 images in the French Alps with mean horizontal/vertical displacement equal to 17.5/-52m. The zoom section on the right highlights the vertical displacement. Measurements regarding the geometric and radiometric dissimilarity between these two scenes are given in Fig. 2.

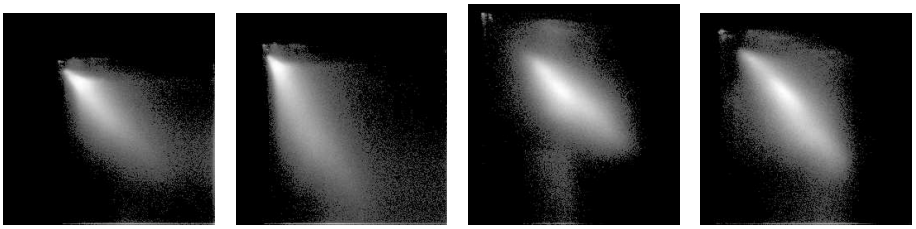

Figure 4: Scattergrams of bands 1 through 4 calculated within the domain of overlap of the image pair shown in Fig. 3. Measurements regarding the geometric and radiometric dissimilarity between these two scenes are given in Fig. 2.

Table 2: Between sensor mean of mean x-y displacements between all overlapping pairs based on DROIs and CROIs.

	DROI			CROI		
	SP4	SP5	IL3	SP4	SP5	IL3
SP4	8.6-7.0	8.4-6.9	6.6-7.4	6.5-7.2	6.9-7.0	6.5-6.7
SP5	6.6-7.4	6.5-7.2	4.4-5.0	4.3-4.8	5.0-5.8	4.6-5.5
IL3	6.9-7.0	6.5-6.7	5.0-5.8	4.6-5.5	4.6-5.4	4.3-5.1

Table 3: Between sensor mean of x-y RMSE displacements between all overlapping pairs based on DROIs and CROIs.

	DROI			CROI		
	SP4	SP5	IL3	SP4	SP5	IL3
SP4	11.5-10.0	11.3-9.9	10.2-10.9	10.1-10.7	10.7-10.7	10.3-10.4
SP5	10.2-10.9	10.1-10.7	6.3-7.3	6.2-7.2	8.3-9.3	7.9-9.1
IL3	10.7-10.7	10.3-10.4	8.3-9.3	7.9-9.1	8.1-8.9	7.7-8.5

Table 4: Between sensor maximum of the mean x-y displacements between all overlapping pairs based on DROIs and CROIs.

	DROI			CROI		
	SP4	SP5	IL3	SP4	SP5	IL3
SP4	111.8-78.3	111.8-82.8	61.4-58.8	61.4-58.7	79.8-70.2	79.8-80.2
SP5	61.4-58.8	61.4-58.7	52.5-50.5	52.5-49.0	67.8-85.0	53.4-85.0
IL3	79.8-70.2	79.8-80.2	67.8-85.0	53.4-85.0	70.8-67.3	67.7-65.4

all countries. However, for almost all countries, there exists at least one pair of images showing a displacement of more than one pixel in either x or y directions. Also, one can observe that the geometric consistency of the within country pairs varies from one country to another. This variability is illustrated in Fig. 5 where the mean horizontal and vertical displacements of all pairs occurring in Iceland and Estonia are plotted.

Displacement measurements between an image originating from a country and all those originating from neighbouring country are presented for each country in appendix A.

5.2 Radiometric consistency

The frequency distribution (histogram) of the correlation values calculated for all overlapping pairs originating from the same sensor or between different sensors are shown in Fig. 6. A bin size of 0.05 has been used for producing these histograms. All intervals include the lower bound and not the upper bound (except the last one that also contains the upper bound). Note that there are many more pairs with a correlation value in the range $[0.95, 1.0]$ when consid-

Table 5: Within country geometric consistency assessment using CROIs.

CC	#pair$_i$	$\overline{\lvert\overline{X}_i\rvert}$	$\overline{\lvert\overline{Y}_i\rvert}$	$\overline{\text{RMSE-}X_i}$	$\overline{\text{RMSE-}Y_i}$	$\lvert\overline{X}_i\rvert_{\max}$	$\lvert\overline{Y}_i\rvert_{\max}$
al	95	10.5	5.8	12.8	8.1	49.4	24.7
at	375	4.4	6.7	7.0	9.4	22.4	45.7
ba	175	3.1	4.6	6.0	7.2	20.9	19.4
be	111	3.0	4.8	6.1	7.8	18.8	22.7
bg	464	7.6	5.3	11.4	8.9	44.5	26.9
ch	189	4.7	6.7	8.8	10.6	24.0	47.8
cs	338	7.3	5.6	10.8	9.4	35.7	30.7
cy	8	2.6	5.5	5.1	7.3	4.6	13.5
cz	263	4.8	3.8	7.4	6.8	20.2	26.0
de	1391	3.9	5.4	7.1	8.4	23.3	44.9
dk	308	4.8	3.7	10.2	9.9	25.6	29.0
ee	156	3.1	3.0	6.4	6.1	17.9	29.8
es	1083	3.7	4.7	6.2	7.4	22.3	37.6
fi	1042	10.4	9.4	13.0	11.9	111.8	58.9
fr	1696	5.1	7.5	8.2	10.6	28.3	53.8
gb	1704	5.5	5.0	10.0	10.4	33.4	30.7
gr	814	6.2	4.9	8.8	7.4	38.5	40.4
hr	158	4.0	5.6	7.6	8.8	19.1	53.2
hu	281	7.0	5.4	11.3	10.4	26.8	31.2
ie	464	5.1	6.9	9.3	11.3	24.5	41.9
is	241	11.3	12.7	15.4	16.8	48.2	78.3
it	1179	6.0	6.7	9.0	9.8	54.1	85.0
li	1	0.6	9.5	3.4	10.6	0.6	9.5
lt	290	5.6	5.6	8.4	8.6	22.6	27.5
lu	13	2.9	4.3	5.2	6.5	6.4	12.2
lv	161	4.4	3.5	6.7	5.8	21.5	14.2
mc	57	8.0	6.0	10.9	9.3	29.8	24.6
me	35	6.0	4.4	8.4	7.5	24.5	15.0
mt	1	9.7	4.5	16.5	25.2	9.7	4.5
ni	81	5.8	6.0	10.7	11.7	23.3	26.4
nl	295	5.0	4.7	11.3	11.0	31.5	31.2
no	1733	6.0	8.4	10.3	11.9	61.4	51.9
pl	841	5.0	3.4	7.9	6.5	26.4	20.2
pt	242	5.1	4.2	7.3	6.5	28.5	36.0
ro	824	7.3	5.2	11.8	10.3	43.7	26.6
se	1304	6.0	7.3	8.1	9.4	43.9	52.2
si	78	4.4	4.7	6.9	7.1	19.6	19.7
sk	138	5.6	3.4	9.3	7.4	27.0	17.7
tr	1828	4.3	4.2	7.1	7.0	34.6	23.9

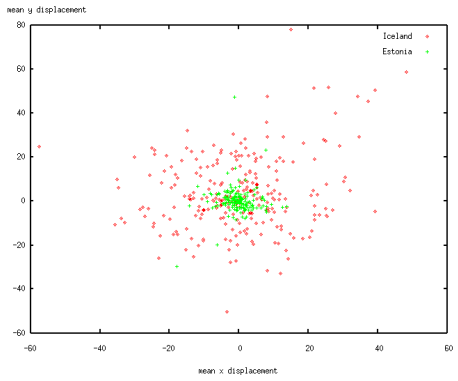

Figure 5: Mean displacements of all pairs of overlapping images occurring in Iceland (red points) and Estonia (green points).

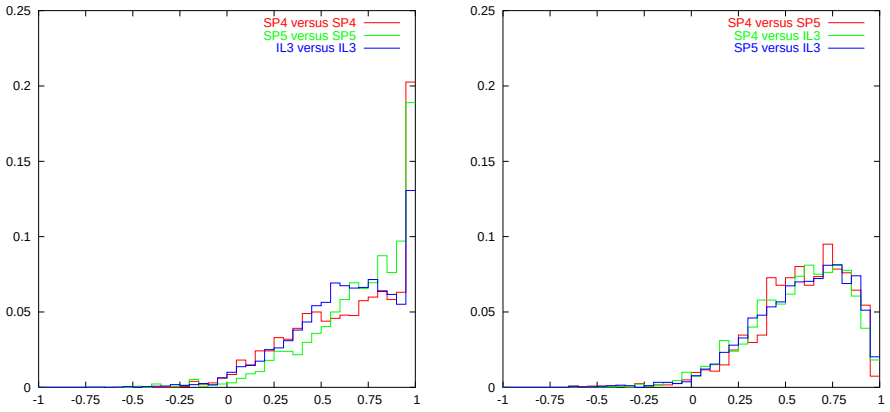

Figure 6: Histogram of the correlation values calculated for all overlapping pairs originating from the same sensor (left) or between different sensors (right). All calculations are based on DROIs.

ering pairs originating from the same sensor. This is mainly due to along path overlapping pairs acquired on the same day, i.e., originating from the same raw image.

Beyond the correlation values, the visual quality of the mosaic depends also on the coefficients of the linear regression computed for the top of atmosphere values. Ideally, the slope parameter should be close to 1 and the offset close to 0.

6 Conclusion

Measurements presented in this report enable to assess whether any given pair of overlapping images are in agreement in both geometry and radiometry. Therefore, when creating a mosaic, a quantitative evaluation of the degree of match

between any pair of adjacent pieces of the mosaic will be straightforward as illustrated in [9]. In particular, a visual representation of the geometric and radiometric consistency will be obtained by setting the boundary of the mosaic pieces to appropriate consistency measurements calculated between the corresponding overlapping image pairs.

Contrary to consistency measurements, accuracy measurements require the availability of a reference data set of known accuracy. Given the unavailability of a reference data set covering the entire territory of the 38 IMAGE-2006 participating countries, accuracy measurements are beyond the scope of this report. Nevertheless, one should keep in mind that inconsistencies revealed by a consistency check always indicate the presence of inaccurate data. For example if the norm of the displacement vector between 2 images is equal to 2 pixels, the minimum of the norms of the two displacement vectors calculated for each image with respect to ground truth is equal to 1 pixel. This 'best' case (given a measured disagreement of 2 pixels between the 2 images) occurs in the unlikely event where each image would be translated by 1 pixel, but in opposite directions with respect to ground truth.

A Between country geometric consistency

Displacement measurements between an image originating from a country and all those originating from neighbouring country are presented for each country hereafter (see tables 6–43). Beware that all country codes used in these tables are referring to the codes used in the data delivered to JRC and therefore depart sometimes from normalised codes, see details in [8].

Table 6: Cross country geometric consistency assessment for **al**.

CC	#pair$_i$	$\overline{\lvert\overline{X}_i\rvert}$	$\overline{\lvert\overline{Y}_i\rvert}$	$\overline{\text{RMSE-}X_i}$	$\overline{\text{RMSE-}Y_i}$	$\lvert\overline{X}_i\rvert_{\max}$	$\lvert\overline{Y}_i\rvert_{\max}$
calculations based on DROIs							
ba	7	5.5	7.4	7.5	10.0	10.6	17.5
cs	64	5.6	4.0	8.4	6.8	27.3	12.7
gr	108	13.0	5.3	15.5	7.6	52.9	21.5
hr	4	2.7	5.9	4.2	7.4	5.0	11.5
it	8	4.3	7.1	9.9	12.3	7.8	14.1
mc	60	9.8	4.1	12.9	7.8	46.3	18.5
me	37	4.8	5.7	7.9	8.5	18.1	17.5
calculations based on CROIs							
cs	45	6.2	3.0	8.7	6.2	19.2	9.7
gr	66	7.6	5.0	11.1	8.7	41.7	28.0
it	8	3.8	7.0	9.9	13.9	8.1	13.9
mc	42	8.9	4.8	11.7	8.5	42.5	18.6
me	26	7.9	4.7	11.3	8.5	19.5	15.8

Table 7: Cross country geometric consistency assessment for **at**.

CC	#pair$_i$	$\overline{\lvert\overline{X}_i\rvert}$	$\overline{\lvert\overline{Y}_i\rvert}$	$\overline{\text{RMSE-}X_i}$	$\overline{\text{RMSE-}Y_i}$	$\lvert\overline{X}_i\rvert_{\max}$	$\lvert\overline{Y}_i\rvert_{\max}$
calculations based on DROIs							
ba	2	10.5	4.2	12.3	6.9	14.3	5.0
ch	55	9.5	10.2	12.0	12.6	26.8	36.7
cz	159	3.9	5.9	6.9	8.7	16.7	23.8
de	188	4.2	4.5	7.2	7.4	21.9	25.7
hr	35	5.7	4.7	7.5	7.2	16.7	10.7
hu	84	6.5	6.4	10.0	10.7	24.2	26.1
it	123	7.4	5.5	10.2	9.0	31.7	21.8
li	11	3.3	1.6	5.9	4.3	11.0	4.6
pl	2	2.6	0.6	4.3	5.1	3.8	0.9
si	113	4.5	5.6	7.0	8.5	17.5	24.2
sk	48	6.2	4.0	11.1	9.9	23.6	15.7
calculations based on CROIs							
ch	32	8.7	7.5	11.1	10.3	26.4	25.3
cz	67	4.2	4.7	6.9	7.5	15.2	22.7
de	113	3.8	3.2	6.3	5.9	19.0	17.8
hr	3	21.6	16.7	27.2	21.4	28.2	21.9
hu	43	5.4	7.0	8.7	10.5	16.6	27.0
it	71	6.2	5.6	8.9	8.6	25.3	23.4
li	8	3.3	4.1	4.1	5.2	5.8	10.0
si	47	3.9	4.9	5.7	7.0	20.7	24.2
sk	16	3.2	8.2	6.2	11.4	13.6	25.0

Table 8: Cross country geometric consistency assessment for **ba**.

CC	#pair$_i$	$\overline{\lvert\overline{X}_i\rvert}$	$\overline{\lvert\overline{Y}_i\rvert}$	$\overline{\text{RMSE-}X_i}$	$\overline{\text{RMSE-}Y_i}$	$\lvert\overline{X}_i\rvert_{\max}$	$\lvert\overline{Y}_i\rvert_{\max}$
calculations based on DROIs							
al	7	5.5	7.4	7.5	10.0	10.6	17.5
at	2	10.5	4.2	12.3	6.9	14.3	5.0
cs	95	3.8	7.8	9.2	12.2	20.6	40.6
hr	207	4.5	5.4	7.8	8.6	28.4	40.6
hu	13	8.7	12.6	16.3	18.0	22.5	32.1
me	48	4.4	5.6	6.6	7.9	20.5	14.9
ro	1	0.0	35.9	8.9	37.1	0.0	35.9
si	10	17.5	7.7	20.0	11.1	47.0	21.1
calculations based on CROIs							
cs	50	3.6	6.4	9.6	11.3	16.0	21.8
hr	151	4.4	5.2	8.5	8.7	27.3	29.1
me	36	4.1	5.7	6.5	8.2	17.2	18.7

Table 9: Cross country geometric consistency assessment for **be**.

CC	#pair$_i$	$\overline{\lvert\overline{X}_i\rvert}$	$\overline{\lvert\overline{Y}_i\rvert}$	$\overline{\text{RMSE-}X_i}$	$\overline{\text{RMSE-}Y_i}$	$\lvert\overline{X}_i\rvert_{\max}$	$\lvert\overline{Y}_i\rvert_{\max}$
calculations based on DROIs							
de	86	3.0	6.6	5.3	9.4	19.0	28.1
fr	134	4.0	5.2	7.5	8.8	21.3	26.1
lu	38	7.5	5.2	9.3	7.7	28.2	18.0
nl	151	3.0	3.5	6.9	7.7	13.6	25.1
calculations based on CROIs							
de	26	2.7	7.8	4.2	9.2	8.9	19.8
fr	75	4.7	6.5	9.1	10.6	21.0	32.2
lu	19	10.2	3.2	11.4	5.6	29.8	9.7
nl	92	3.0	3.3	8.0	8.6	15.2	15.4

Table 10: Cross country geometric consistency assessment for **bg**.

CC	#pair$_i$	$\overline{\lvert\overline{X}_i\rvert}$	$\overline{\lvert\overline{Y}_i\rvert}$	$\overline{\text{RMSE-}X_i}$	$\overline{\text{RMSE-}Y_i}$	$\lvert\overline{X}_i\rvert_{\max}$	$\lvert\overline{Y}_i\rvert_{\max}$
calculations based on DROIs							
cs	121	10.7	7.2	13.1	9.8	35.8	26.8
gr	176	6.3	7.5	9.2	9.9	27.3	26.5
mc	70	6.4	5.9	8.8	8.2	28.4	23.7
ro	194	8.7	8.2	16.5	15.1	54.8	39.9
tr	64	8.1	5.1	11.1	8.3	26.3	14.5
calculations based on CROIs							
cs	69	10.6	7.7	12.3	9.7	29.7	25.8
gr	81	6.8	5.3	8.6	7.5	27.2	26.2
mc	41	4.1	3.5	5.7	5.9	12.6	16.7
ro	97	8.5	8.0	20.8	17.7	50.7	37.6
tr	36	6.3	5.7	8.0	7.3	20.4	17.9

Table 11: Cross country geometric consistency assessment for **ch**.

CC	#pair$_i$	$\overline{\lvert\overline{X}_i\rvert}$	$\overline{\lvert\overline{Y}_i\rvert}$	$\overline{\text{RMSE-}X_i}$	$\overline{\text{RMSE-}Y_i}$	$\lvert\overline{X}_i\rvert_{\max}$	$\lvert\overline{Y}_i\rvert_{\max}$
calculations based on DROIs							
at	55	9.5	10.2	12.0	12.6	26.8	36.7
de	125	7.6	7.8	10.0	10.9	25.8	36.7
fr	82	7.8	9.3	10.3	12.4	30.1	33.4
it	173	8.8	13.0	13.0	16.3	31.7	41.4
li	29	9.9	8.5	11.7	11.2	23.5	34.0
calculations based on CROIs							
at	32	8.7	7.5	11.1	10.3	26.4	25.3
de	47	4.8	5.1	8.8	9.3	13.8	18.3
fr	69	7.8	9.5	10.0	12.8	30.4	36.2
it	130	6.5	10.2	11.4	13.7	19.3	33.8
li	10	8.2	9.3	10.1	11.1	17.5	25.5

Table 12: Cross country geometric consistency assessment for **cs**.

CC	#pair$_i$	$\overline{\lvert\overline{X}_i\rvert}$	$\overline{\lvert\overline{Y}_i\rvert}$	$\overline{\text{RMSE-}X_i}$	$\overline{\text{RMSE-}Y_i}$	$\lvert\overline{X}_i\rvert_{\max}$	$\lvert\overline{Y}_i\rvert_{\max}$
calculations based on DROIs							
al	64	5.6	4.0	8.4	6.8	27.3	12.7
ba	95	3.8	7.8	9.2	12.2	20.6	40.6
bg	121	10.7	7.2	13.1	9.8	35.8	26.8
gr	5	6.0	14.6	7.9	16.6	9.2	19.9
hr	47	6.0	8.8	12.3	15.2	27.5	53.4
hu	69	7.3	6.2	12.8	11.7	27.7	18.2
mc	62	6.8	5.2	10.0	8.3	28.4	23.7
me	78	4.4	4.9	6.7	7.3	18.7	14.6
ro	142	9.0	7.1	13.1	11.4	26.8	50.7
calculations based on CROIs							
al	45	6.2	3.0	8.7	6.2	19.2	9.7
ba	50	3.6	6.4	9.6	11.3	16.0	21.8
bg	69	10.6	7.7	12.3	9.7	29.7	25.8
hr	36	5.2	11.2	11.5	16.0	19.9	53.2
hu	28	6.7	5.3	10.2	9.6	22.5	13.1
mc	38	6.8	4.9	9.1	7.5	26.1	22.4
me	76	4.4	4.8	6.6	7.1	20.9	14.6
ro	66	7.4	5.4	12.5	10.9	24.8	19.7

Table 13: Cross country geometric consistency assessment for **cy**.

CC	#pair$_i$	$\overline{\lvert\overline{X}_i\rvert}$	$\overline{\lvert\overline{Y}_i\rvert}$	$\overline{\text{RMSE-}X_i}$	$\overline{\text{RMSE-}Y_i}$	$\lvert\overline{X}_i\rvert_{\max}$	$\lvert\overline{Y}_i\rvert_{\max}$
calculations based on DROIs							
tr	1	23.9	7.2	23.9	8.0	23.9	7.2
calculations based on CROIs							

Table 14: Cross country geometric consistency assessment for **cz**.

CC	#pair$_i$	$\overline{\lvert\overline{X}_i\rvert}$	$\overline{\lvert\overline{Y}_i\rvert}$	$\overline{\text{RMSE-}X_i}$	$\overline{\text{RMSE-}Y_i}$	$\lvert\overline{X}_i\rvert_{\max}$	$\lvert\overline{Y}_i\rvert_{\max}$
calculations based on DROIs							
at	159	3.9	5.9	6.9	8.7	16.7	23.8
de	179	4.0	4.4	6.5	7.3	21.8	23.8
hu	14	6.0	7.1	12.9	12.4	15.1	16.3
pl	176	4.8	3.7	7.7	6.7	28.3	17.1
sk	53	4.4	2.2	8.6	6.8	20.7	8.3
calculations based on CROIs							
at	67	4.2	4.7	6.9	7.5	15.2	22.7
de	121	3.5	4.5	5.2	6.3	15.4	17.3
pl	85	4.2	3.5	6.5	6.1	27.0	20.4
sk	32	5.4	2.3	6.8	4.1	18.8	5.4

Table 15: Cross country geometric consistency assessment for **de**.

CC	#pair$_i$	$\overline{\lvert X_i \rvert}$	$\overline{\lvert Y_i \rvert}$	$\overline{\text{RMSE-}X_i}$	$\overline{\text{RMSE-}Y_i}$	$\lvert \overline{X}_i \rvert_{\max}$	$\lvert \overline{Y}_i \rvert_{\max}$
calculations based on DROIs							
at	188	4.2	4.5	7.2	7.4	21.9	25.7
be	86	3.0	6.6	5.3	9.4	19.0	28.1
ch	125	7.6	7.8	10.0	10.9	25.8	36.7
cz	179	4.0	4.4	6.5	7.3	21.8	23.8
dk	138	4.7	4.9	12.3	12.6	23.5	22.9
fr	214	4.5	6.4	7.0	9.1	18.7	33.2
it	51	8.9	10.5	12.4	12.8	26.6	49.5
li	23	4.0	8.6	6.6	10.7	16.4	27.1
lu	42	4.0	5.8	7.0	8.8	18.1	21.4
nl	205	3.6	4.7	8.6	9.4	19.7	34.5
pl	116	4.1	4.6	8.1	8.2	22.0	22.0
se	2	5.1	17.6	8.8	21.3	9.3	17.6
si	1	9.5	12.8	12.5	16.5	9.5	12.8
calculations based on CROIs							
at	113	3.8	3.2	6.3	5.9	19.0	17.8
be	26	2.7	7.8	4.2	9.2	8.9	19.8
ch	47	4.8	5.1	8.8	9.3	13.8	18.3
cz	121	3.5	4.5	5.2	6.3	15.4	17.3
dk	54	4.7	6.5	16.2	15.7	22.7	17.8
fr	118	4.5	5.1	6.9	8.7	20.2	23.6
lu	28	4.2	5.6	6.4	8.3	18.2	17.8
nl	118	4.1	4.4	11.1	11.4	39.8	21.7
pl	60	4.3	4.2	7.7	7.3	26.1	17.7
se	1	1.1	12.3	7.7	30.2	1.1	12.3

Table 16: Cross country geometric consistency assessment for **dk**.

CC	#pair$_i$	$\overline{\lvert X_i \rvert}$	$\overline{\lvert Y_i \rvert}$	$\overline{\text{RMSE-}X_i}$	$\overline{\text{RMSE-}Y_i}$	$\lvert \overline{X}_i \rvert_{\max}$	$\lvert \overline{Y}_i \rvert_{\max}$
calculations based on DROIs							
de	138	4.7	4.9	12.3	12.6	23.5	22.9
no	4	5.2	19.3	14.4	20.7	7.9	22.1
se	68	7.5	9.1	13.8	14.2	48.7	41.8
calculations based on CROIs							
de	54	4.7	6.5	16.2	15.7	22.7	17.8
se	22	6.2	11.1	14.3	17.1	27.2	26.3

Table 17: Cross country geometric consistency assessment for **ee**.

CC	#pair$_i$	$\overline{\lvert\overline{X}_i\rvert}$	$\overline{\lvert\overline{Y}_i\rvert}$	$\overline{\text{RMSE-}X_i}$	$\overline{\text{RMSE-}Y_i}$	$\lvert\overline{X}_i\rvert_{\max}$	$\lvert\overline{Y}_i\rvert_{\max}$
calculations based on DROIs							
fi	31	12.8	9.4	14.8	11.9	34.5	24.1
lt	3	4.4	7.8	6.9	9.2	9.3	8.4
lv	68	3.8	3.6	6.4	6.1	19.3	12.2
calculations based on CROIs							
fi	14	8.7	5.6	10.4	6.9	25.8	20.3
lv	42	3.7	3.8	6.9	7.2	19.7	13.2

Table 18: Cross country geometric consistency assessment for **es**.

CC	#pair$_i$	$\overline{\lvert\overline{X}_i\rvert}$	$\overline{\lvert\overline{Y}_i\rvert}$	$\overline{\text{RMSE-}X_i}$	$\overline{\text{RMSE-}Y_i}$	$\lvert\overline{X}_i\rvert_{\max}$	$\lvert\overline{Y}_i\rvert_{\max}$
calculations based on DROIs							
fr	208	3.7	6.2	6.7	9.2	23.3	25.3
pt	219	4.1	3.3	6.3	5.6	21.7	19.1
calculations based on CROIs							
fr	120	2.9	6.3	6.0	9.1	15.2	24.9
pt	133	4.0	2.9	5.1	4.5	17.8	16.7

Table 19: Cross country geometric consistency assessment for **fi**.

CC	#pair$_i$	$\overline{\lvert\overline{X}_i\rvert}$	$\overline{\lvert\overline{Y}_i\rvert}$	$\overline{\text{RMSE-}X_i}$	$\overline{\text{RMSE-}Y_i}$	$\lvert\overline{X}_i\rvert_{\max}$	$\lvert\overline{Y}_i\rvert_{\max}$
calculations based on DROIs							
ee	31	12.8	9.4	14.8	11.9	34.5	24.1
no	186	13.0	12.1	16.5	14.7	79.0	70.2
se	224	15.8	16.0	18.1	17.9	75.5	63.2
calculations based on CROIs							
ee	14	8.7	5.6	10.4	6.9	25.8	20.3
no	103	8.3	6.9	11.1	9.9	37.4	38.8
se	155	13.0	16.0	14.9	18.1	47.8	82.8

Table 20: Cross country geometric consistency assessment for **fr**.

CC	#pair$_i$	$\overline{\lvert\overline{X}_i\rvert}$	$\overline{\lvert\overline{Y}_i\rvert}$	$\overline{\text{RMSE-}X_i}$	$\overline{\text{RMSE-}Y_i}$	$\lvert\overline{X}_i\rvert_{\max}$	$\lvert\overline{Y}_i\rvert_{\max}$
calculations based on DROIs							
be	134	4.0	5.2	7.5	8.8	21.3	26.1
ch	82	7.8	9.3	10.3	12.4	30.1	33.4
de	214	4.5	6.4	7.0	9.1	18.7	33.2
es	208	3.7	6.2	6.7	9.2	23.3	25.3
gb	5	5.3	10.9	12.6	17.6	10.1	22.0
it	197	9.3	16.6	12.5	19.6	57.1	54.8
lu	39	5.4	4.3	8.0	7.2	22.6	17.3
nl	20	3.3	4.1	9.4	10.4	8.5	17.0
calculations based on CROIs							
be	75	4.7	6.5	9.1	10.6	21.0	32.2
ch	69	7.8	9.5	10.0	12.8	30.4	36.2
de	118	4.5	5.1	6.9	8.7	20.2	23.6
es	120	2.9	6.3	6.0	9.1	15.2	24.9
gb	1	4.6	19.0	10.3	28.2	4.6	19.0
it	96	9.7	18.2	12.4	20.4	32.6	52.6
lu	22	6.4	4.4	8.0	6.1	22.2	13.4
nl	6	2.6	5.6	29.3	28.2	5.8	12.2

Table 21: Cross country geometric consistency assessment for **gb**.

CC	#pair$_i$	$\overline{\lvert\overline{X}_i\rvert}$	$\overline{\lvert\overline{Y}_i\rvert}$	$\overline{\text{RMSE-}X_i}$	$\overline{\text{RMSE-}Y_i}$	$\lvert\overline{X}_i\rvert_{\max}$	$\lvert\overline{Y}_i\rvert_{\max}$
calculations based on DROIs							
fr	5	5.3	10.9	12.6	17.6	10.1	22.0
ie	173	5.9	5.7	10.6	11.2	23.0	33.1
ni	276	5.3	5.0	9.8	10.3	23.3	26.4
calculations based on CROIs							
fr	1	4.6	19.0	10.3	28.2	4.6	19.0
ie	79	6.1	4.8	10.3	10.1	25.4	20.0
ni	265	5.4	5.2	9.9	10.5	23.3	26.4

Table 22: Cross country geometric consistency assessment for **gr**.

CC	#pair$_i$	$\overline{\lvert\overline{X}_i\rvert}$	$\overline{\lvert\overline{Y}_i\rvert}$	$\overline{\text{RMSE-}X_i}$	$\overline{\text{RMSE-}Y_i}$	$\lvert\overline{X}_i\rvert_{\max}$	$\lvert\overline{Y}_i\rvert_{\max}$
calculations based on DROIs							
al	108	13.0	5.3	15.5	7.6	52.9	21.5
bg	176	6.3	7.5	9.2	9.9	27.3	26.5
cs	5	6.0	14.6	7.9	16.6	9.2	19.9
it	2	4.0	6.8	9.3	10.5	6.5	11.8
mc	153	8.7	6.4	11.4	9.5	52.8	27.0
tr	198	11.5	6.4	14.4	9.2	67.8	25.4
calculations based on CROIs							
al	66	7.6	5.0	11.1	8.7	41.7	28.0
bg	81	6.8	5.3	8.6	7.5	27.2	26.2
it	2	3.1	5.6	7.9	10.0	5.3	10.4
mc	79	7.2	5.8	9.8	8.7	25.2	25.8
tr	90	7.1	5.2	10.7	9.3	51.8	19.6

Table 23: Cross country geometric consistency assessment for **hr**.

CC	#pair$_i$	$\overline{\lvert\overline{X}_i\rvert}$	$\overline{\lvert\overline{Y}_i\rvert}$	$\overline{\text{RMSE-}X_i}$	$\overline{\text{RMSE-}Y_i}$	$\lvert\overline{X}_i\rvert_{\max}$	$\lvert\overline{Y}_i\rvert_{\max}$
calculations based on DROIs							
al	4	2.7	5.9	4.2	7.4	5.0	11.5
at	35	5.7	4.7	7.5	7.2	16.7	10.7
ba	207	4.5	5.4	7.8	8.6	28.4	40.6
cs	47	6.0	8.8	12.3	15.2	27.5	53.4
hu	65	7.3	9.4	11.3	13.6	26.9	40.6
it	25	7.1	7.0	9.6	9.8	36.3	21.5
me	22	3.0	3.0	5.4	6.0	7.5	11.4
si	97	5.2	4.5	8.1	7.3	23.2	17.4
calculations based on CROIs							
at	3	21.6	16.7	27.2	21.4	28.2	21.9
ba	151	4.4	5.2	8.5	8.7	27.3	29.1
cs	36	5.2	11.2	11.5	16.0	19.9	53.2
hu	34	7.4	10.6	12.7	15.2	20.4	30.7
it	7	14.2	11.8	26.6	15.8	28.2	17.7
me	10	4.7	2.1	6.1	4.5	13.2	4.8
si	59	3.4	3.6	5.9	5.6	14.6	10.3

Table 24: Cross country geometric consistency assessment for **hu**.

CC	#pair$_i$	$\overline{\lvert\overline{X}_i\rvert}$	$\overline{\lvert\overline{Y}_i\rvert}$	$\overline{\text{RMSE-}X_i}$	$\overline{\text{RMSE-}Y_i}$	$\lvert\overline{X}_i\rvert_{\max}$	$\lvert\overline{Y}_i\rvert_{\max}$
calculations based on DROIs							
at	84	6.5	6.4	10.0	10.7	24.2	26.1
ba	13	8.7	12.6	16.3	18.0	22.5	32.1
cs	69	7.3	6.2	12.8	11.7	27.7	18.2
cz	14	6.0	7.1	12.9	12.4	15.1	16.3
hr	65	7.3	9.4	11.3	13.6	26.9	40.6
pl	16	4.4	4.6	8.2	8.4	13.2	17.9
ro	81	6.1	7.9	11.8	13.6	24.7	55.2
si	32	7.1	7.7	10.1	11.7	23.4	24.4
sk	157	6.1	5.4	10.9	10.3	23.9	21.3
calculations based on CROIs							
at	43	5.4	7.0	8.7	10.5	16.6	27.0
cs	28	6.7	5.3	10.2	9.6	22.5	13.1
hr	34	7.4	10.6	12.7	15.2	20.4	30.7
pl	3	4.5	4.0	8.1	7.4	9.9	8.4
ro	42	5.0	5.4	11.1	9.6	16.3	20.2
si	18	5.8	11.1	8.4	13.0	17.4	25.9
sk	98	6.1	5.4	11.4	10.5	24.3	23.2

Table 25: Cross country geometric consistency assessment for **ie**.

CC	#pair$_i$	$\overline{\lvert\overline{X}_i\rvert}$	$\overline{\lvert\overline{Y}_i\rvert}$	$\overline{\text{RMSE-}X_i}$	$\overline{\text{RMSE-}Y_i}$	$\lvert\overline{X}_i\rvert_{\max}$	$\lvert\overline{Y}_i\rvert_{\max}$
calculations based on DROIs							
gb	173	5.9	5.7	10.6	11.2	23.0	33.1
ni	113	5.8	5.6	10.5	11.1	21.4	30.1
calculations based on CROIs							
gb	79	6.1	4.8	10.3	10.1	25.4	20.0
ni	56	6.7	5.2	11.5	11.2	25.4	20.0

Table 26: Cross country geometric consistency assessment for **it**.

CC	#pair$_i$	$\overline{\lvert\overline{X}_i\rvert}$	$\overline{\lvert\overline{Y}_i\rvert}$	$\overline{\text{RMSE-}X_i}$	$\overline{\text{RMSE-}Y_i}$	$\lvert\overline{X}_i\rvert_{\max}$	$\lvert\overline{Y}_i\rvert_{\max}$
calculations based on DROIs							
al	8	4.3	7.1	9.9	12.3	7.8	14.1
at	123	7.4	5.5	10.2	9.0	31.7	21.8
ch	173	8.8	13.0	13.0	16.3	31.7	41.4
de	51	8.9	10.5	12.4	12.8	26.6	49.5
fr	197	9.3	16.6	12.5	19.6	57.1	54.8
gr	2	4.0	6.8	9.3	10.5	6.5	11.8
hr	25	7.1	7.0	9.6	9.8	36.3	21.5
li	6	10.0	11.7	13.1	13.2	22.0	31.0
mt	1	26.4	67.3	26.4	68.4	26.4	67.3
si	45	6.0	5.2	8.9	7.9	20.2	13.5
calculations based on CROIs							
al	8	3.8	7.0	9.9	13.9	8.1	13.9
at	71	6.2	5.6	8.9	8.6	25.3	23.4
ch	130	6.5	10.2	11.4	13.7	19.3	33.8
fr	96	9.7	18.2	12.4	20.4	32.6	52.6
gr	2	3.1	5.6	7.9	10.0	5.3	10.4
hr	7	14.2	11.8	26.6	15.8	28.2	17.7
si	32	6.3	5.6	8.6	7.5	18.6	15.8

Table 27: Cross country geometric consistency assessment for **li**.

CC	#pair$_i$	$\overline{\lvert\overline{X}_i\rvert}$	$\overline{\lvert\overline{Y}_i\rvert}$	$\overline{\text{RMSE-}X_i}$	$\overline{\text{RMSE-}Y_i}$	$\lvert\overline{X}_i\rvert_{\max}$	$\lvert\overline{Y}_i\rvert_{\max}$
calculations based on DROIs							
at	11	3.3	1.6	5.9	4.3	11.0	4.6
ch	29	9.9	8.5	11.7	11.2	23.5	34.0
de	23	4.0	8.6	6.6	10.7	16.4	27.1
it	6	10.0	11.7	13.1	13.2	22.0	31.0
calculations based on CROIs							
at	8	3.3	4.1	4.1	5.2	5.8	10.0
ch	10	8.2	9.3	10.1	11.1	17.5	25.5

Table 28: Cross country geometric consistency assessment for **lt**.

CC	#pair$_i$	$\overline{\lvert\overline{X}_i\rvert}$	$\overline{\lvert\overline{Y}_i\rvert}$	$\overline{\text{RMSE-}X_i}$	$\overline{\text{RMSE-}Y_i}$	$\lvert\overline{X}_i\rvert_{\max}$	$\lvert\overline{Y}_i\rvert_{\max}$
calculations based on DROIs							
ee	3	4.4	7.8	6.9	9.2	9.3	8.4
lv	144	4.2	3.9	6.9	6.7	21.3	20.8
pl	99	7.0	5.1	9.3	7.8	46.9	17.6
calculations based on CROIs							
lv	101	4.7	4.4	7.0	6.9	21.4	21.2
pl	71	6.0	5.6	8.0	7.8	22.3	18.6

Table 29: Cross country geometric consistency assessment for **lu**.

CC	#pair$_i$	$\overline{\lvert X_i \rvert}$	$\overline{\lvert Y_i \rvert}$	$\overline{\text{RMSE-}X_i}$	$\overline{\text{RMSE-}Y_i}$	$\lvert X_i \rvert_{\max}$	$\lvert Y_i \rvert_{\max}$
calculations based on DROIs							
be	38	7.5	5.2	9.3	7.7	28.2	18.0
de	42	4.0	5.8	7.0	8.8	18.1	21.4
fr	39	5.4	4.3	8.0	7.2	22.6	17.3
nl	1	7.1	17.8	8.2	19.1	7.1	17.8
calculations based on CROIs							
be	19	10.2	3.2	11.4	5.6	29.8	9.7
de	28	4.2	5.6	6.4	8.3	18.2	17.8
fr	22	6.4	4.4	8.0	6.1	22.2	13.4

Table 30: Cross country geometric consistency assessment for **lv**.

CC	#pair$_i$	$\overline{\lvert X_i \rvert}$	$\overline{\lvert Y_i \rvert}$	$\overline{\text{RMSE-}X_i}$	$\overline{\text{RMSE-}Y_i}$	$\lvert X_i \rvert_{\max}$	$\lvert Y_i \rvert_{\max}$
calculations based on DROIs							
ee	68	3.8	3.6	6.4	6.1	19.3	12.2
lt	144	4.2	3.9	6.9	6.7	21.3	20.8
calculations based on CROIs							
ee	42	3.7	3.8	6.9	7.2	19.7	13.2
lt	101	4.7	4.4	7.0	6.9	21.4	21.2

Table 31: Cross country geometric consistency assessment for **mc**.

CC	#pair$_i$	$\overline{\lvert X_i \rvert}$	$\overline{\lvert Y_i \rvert}$	$\overline{\text{RMSE-}X_i}$	$\overline{\text{RMSE-}Y_i}$	$\lvert X_i \rvert_{\max}$	$\lvert Y_i \rvert_{\max}$
calculations based on DROIs							
al	60	9.8	4.1	12.9	7.8	46.3	18.5
bg	70	6.4	5.9	8.8	8.2	28.4	23.7
cs	62	6.8	5.2	10.0	8.3	28.4	23.7
gr	153	8.7	6.4	11.4	9.5	52.8	27.0
me	1	4.1	5.1	6.3	6.5	4.1	5.1
calculations based on CROIs							
al	42	8.9	4.8	11.7	8.5	42.5	18.6
bg	41	4.1	3.5	5.7	5.9	12.6	16.7
cs	38	6.8	4.9	9.1	7.5	26.1	22.4
gr	79	7.2	5.8	9.8	8.7	25.2	25.8

Table 32: Cross country geometric consistency assessment for **me**.

CC	#pair$_i$	$\overline{\lvert\overline{X}_i\rvert}$	$\overline{\lvert\overline{Y}_i\rvert}$	$\overline{\text{RMSE-}X_i}$	$\overline{\text{RMSE-}Y_i}$	$\lvert\overline{X}_i\rvert_{\max}$	$\lvert\overline{Y}_i\rvert_{\max}$
calculations based on DROIs							
al	37	4.8	5.7	7.9	8.5	18.1	17.5
ba	48	4.4	5.6	6.6	7.9	20.5	14.9
cs	78	4.4	4.9	6.7	7.3	18.7	14.6
hr	22	3.0	3.0	5.4	6.0	7.5	11.4
mc	1	4.1	5.1	6.3	6.5	4.1	5.1
calculations based on CROIs							
al	26	7.9	4.7	11.3	8.5	19.5	15.8
ba	36	4.1	5.7	6.5	8.2	17.2	18.7
cs	76	4.4	4.8	6.6	7.1	20.9	14.6
hr	10	4.7	2.1	6.1	4.5	13.2	4.8

Table 33: Cross country geometric consistency assessment for **mt**.

CC	#pair$_i$	$\overline{\lvert\overline{X}_i\rvert}$	$\overline{\lvert\overline{Y}_i\rvert}$	$\overline{\text{RMSE-}X_i}$	$\overline{\text{RMSE-}Y_i}$	$\lvert\overline{X}_i\rvert_{\max}$	$\lvert\overline{Y}_i\rvert_{\max}$
calculations based on DROIs							
it	1	26.4	67.3	26.4	68.4	26.4	67.3
calculations based on CROIs							

Table 34: Cross country geometric consistency assessment for **ni**.

CC	#pair$_i$	$\overline{\lvert\overline{X}_i\rvert}$	$\overline{\lvert\overline{Y}_i\rvert}$	$\overline{\text{RMSE-}X_i}$	$\overline{\text{RMSE-}Y_i}$	$\lvert\overline{X}_i\rvert_{\max}$	$\lvert\overline{Y}_i\rvert_{\max}$
calculations based on DROIs							
gb	276	5.3	5.0	9.8	10.3	23.3	26.4
ie	113	5.8	5.6	10.5	11.1	21.4	30.1
calculations based on CROIs							
gb	265	5.4	5.2	9.9	10.5	23.3	26.4
ie	56	6.7	5.2	11.5	11.2	25.4	20.0

Table 35: Cross country geometric consistency assessment for **nl**.

CC	#pair$_i$	$\overline{\lvert\overline{X}_i\rvert}$	$\overline{\lvert\overline{Y}_i\rvert}$	$\overline{\text{RMSE-}X_i}$	$\overline{\text{RMSE-}Y_i}$	$\lvert\overline{X}_i\rvert_{\max}$	$\lvert\overline{Y}_i\rvert_{\max}$
calculations based on DROIs							
be	151	3.0	3.5	6.9	7.7	13.6	25.1
de	205	3.6	4.7	8.6	9.4	19.7	34.5
fr	20	3.3	4.1	9.4	10.4	8.5	17.0
lu	1	7.1	17.8	8.2	19.1	7.1	17.8
calculations based on CROIs							
be	92	3.0	3.3	8.0	8.6	15.2	15.4
de	118	4.1	4.4	11.1	11.4	39.8	21.7
fr	6	2.6	5.6	29.3	28.2	5.8	12.2

Table 36: Cross country geometric consistency assessment for **no**.

CC	#pair$_i$	$\overline{\lvert\overline{X}_i\rvert}$	$\overline{\lvert\overline{Y}_i\rvert}$	$\overline{\text{RMSE-}X_i}$	$\overline{\text{RMSE-}Y_i}$	$\lvert\overline{X}_i\rvert_{\max}$	$\lvert\overline{Y}_i\rvert_{\max}$
calculations based on DROIs							
dk	4	5.2	19.3	14.4	20.7	7.9	22.1
fi	186	13.0	12.1	16.5	14.7	79.0	70.2
se	631	10.8	11.4	14.9	14.3	77.5	53.1
calculations based on CROIs							
fi	103	8.3	6.9	11.1	9.9	37.4	38.8
se	343	9.4	10.7	12.8	13.1	67.7	49.4

Table 37: Cross country geometric consistency assessment for **pl**.

CC	#pair$_i$	$\overline{\lvert\overline{X}_i\rvert}$	$\overline{\lvert\overline{Y}_i\rvert}$	$\overline{\text{RMSE-}X_i}$	$\overline{\text{RMSE-}Y_i}$	$\lvert\overline{X}_i\rvert_{\max}$	$\lvert\overline{Y}_i\rvert_{\max}$
calculations based on DROIs							
at	2	2.6	0.6	4.3	5.1	3.8	0.9
cz	176	4.8	3.7	7.7	6.7	28.3	17.1
de	116	4.1	4.6	8.1	8.2	22.0	22.0
hu	16	4.4	4.6	8.2	8.4	13.2	17.9
lt	99	7.0	5.1	9.3	7.8	46.9	17.6
ro	4	6.5	2.1	11.3	8.3	10.7	5.5
sk	136	5.3	3.1	7.9	6.1	26.9	12.0
calculations based on CROIs							
cz	85	4.2	3.5	6.5	6.1	27.0	20.4
de	60	4.3	4.2	7.7	7.3	26.1	17.7
hu	3	4.5	4.0	8.1	7.4	9.9	8.4
lt	71	6.0	5.6	8.0	7.8	22.3	18.6
ro	2	6.1	2.2	8.7	5.2	8.3	3.5
sk	88	4.9	3.0	6.9	5.5	22.5	12.7

Table 38: Cross country geometric consistency assessment for **pt**.

CC	#pair$_i$	$\overline{\lvert\overline{X}_i\rvert}$	$\overline{\lvert\overline{Y}_i\rvert}$	$\overline{\text{RMSE-}X_i}$	$\overline{\text{RMSE-}Y_i}$	$\lvert\overline{X}_i\rvert_{\max}$	$\lvert\overline{Y}_i\rvert_{\max}$
calculations based on DROIs							
es	219	4.1	3.3	6.3	5.6	21.7	19.1
calculations based on CROIs							
es	133	4.0	2.9	5.1	4.5	17.8	16.7

Table 39: Cross country geometric consistency assessment for **ro**.

CC	#pair$_i$	$\overline{\lvert\overline{X}_i\rvert}$	$\overline{\lvert\overline{Y}_i\rvert}$	$\overline{\text{RMSE-}X_i}$	$\overline{\text{RMSE-}Y_i}$	$\lvert\overline{X}_i\rvert_{\max}$	$\lvert\overline{Y}_i\rvert_{\max}$
calculations based on DROIs							
ba	1	0.0	35.9	8.9	37.1	0.0	35.9
bg	194	8.7	8.2	16.5	15.1	54.8	39.9
cs	142	9.0	7.1	13.1	11.4	26.8	50.7
hu	81	6.1	7.9	11.8	13.6	24.7	55.2
pl	4	6.5	2.1	11.3	8.3	10.7	5.5
sk	3	2.9	3.4	7.8	8.5	6.3	6.1
calculations based on CROIs							
bg	97	8.5	8.0	20.8	17.7	50.7	37.6
cs	66	7.4	5.4	12.5	10.9	24.8	19.7
hu	42	5.0	5.4	11.1	9.6	16.3	20.2
pl	2	6.1	2.2	8.7	5.2	8.3	3.5

Table 40: Cross country geometric consistency assessment for **se**.

CC	#pair$_i$	$\overline{\lvert\overline{X}_i\rvert}$	$\overline{\lvert\overline{Y}_i\rvert}$	$\overline{\text{RMSE-}X_i}$	$\overline{\text{RMSE-}Y_i}$	$\lvert\overline{X}_i\rvert_{\max}$	$\lvert\overline{Y}_i\rvert_{\max}$
calculations based on DROIs							
de	2	5.1	17.6	8.8	21.3	9.3	17.6
dk	68	7.5	9.1	13.8	14.2	48.7	41.8
fi	224	15.8	16.0	18.1	17.9	75.5	63.2
no	631	10.8	11.4	14.9	14.3	77.5	53.1
calculations based on CROIs							
de	1	1.1	12.3	7.7	30.2	1.1	12.3
dk	22	6.2	11.1	14.3	17.1	27.2	26.3
fi	155	13.0	16.0	14.9	18.1	47.8	82.8
no	343	9.4	10.7	12.8	13.1	67.7	49.4

Table 41: Cross country geometric consistency assessment for **si**.

CC	#pair$_i$	$\overline{\lvert\overline{X}_i\rvert}$	$\overline{\lvert\overline{Y}_i\rvert}$	$\overline{\text{RMSE-}X_i}$	$\overline{\text{RMSE-}Y_i}$	$\lvert\overline{X}_i\rvert_{\max}$	$\lvert\overline{Y}_i\rvert_{\max}$
calculations based on DROIs							
at	113	4.5	5.6	7.0	8.5	17.5	24.2
ba	10	17.5	7.7	20.0	11.1	47.0	21.1
de	1	9.5	12.8	12.5	16.5	9.5	12.8
hr	97	5.2	4.5	8.1	7.3	23.2	17.4
hu	32	7.1	7.7	10.1	11.7	23.4	24.4
it	45	6.0	5.2	8.9	7.9	20.2	13.5
calculations based on CROIs							
at	47	3.9	4.9	5.7	7.0	20.7	24.2
hr	59	3.4	3.6	5.9	5.6	14.6	10.3
hu	18	5.8	11.1	8.4	13.0	17.4	25.9
it	32	6.3	5.6	8.6	7.5	18.6	15.8

Table 42: Cross country geometric consistency assessment for **sk**.

CC	#pair$_i$	$\overline{\lvert\overline{X}_i\rvert}$	$\overline{\lvert\overline{Y}_i\rvert}$	$\overline{\text{RMSE-}X_i}$	$\overline{\text{RMSE-}Y_i}$	$\lvert\overline{X}_i\rvert_{\max}$	$\lvert\overline{Y}_i\rvert_{\max}$
calculations based on DROIs							
at	48	6.2	4.0	11.1	9.9	23.6	15.7
cz	53	4.4	2.2	8.6	6.8	20.7	8.3
hu	157	6.1	5.4	10.9	10.3	23.9	21.3
pl	136	5.3	3.1	7.9	6.1	26.9	12.0
ro	3	2.9	3.4	7.8	8.5	6.3	6.1
calculations based on CROIs							
at	16	3.2	8.2	6.2	11.4	13.6	25.0
cz	32	5.4	2.3	6.8	4.1	18.8	5.4
hu	98	6.1	5.4	11.4	10.5	24.3	23.2
pl	88	4.9	3.0	6.9	5.5	22.5	12.7

Table 43: Cross country geometric consistency assessment for **tr**.

CC	#pair$_i$	$\overline{\lvert\overline{X}_i\rvert}$	$\overline{\lvert\overline{Y}_i\rvert}$	$\overline{\text{RMSE-}X_i}$	$\overline{\text{RMSE-}Y_i}$	$\lvert\overline{X}_i\rvert_{\max}$	$\lvert\overline{Y}_i\rvert_{\max}$
calculations based on DROIs							
bg	64	8.1	5.1	11.1	8.3	26.3	14.5
cy	1	23.9	7.2	23.9	8.0	23.9	7.2
gr	198	11.5	6.4	14.4	9.2	67.8	25.4
calculations based on CROIs							
bg	36	6.3	5.7	8.0	7.3	20.4	17.9
gr	90	7.1	5.2	10.7	9.3	51.8	19.6

References

[1] D. Barnea and H. Silverman. A class of algorithms for fast digital registration. *IEEE Transactions on Computers*, C-21:179–186, 1972.

[2] V. Dvorchenko. Bounds on (deterministic) correlation functions with applications to registration. *IEEE Transactions on Pattern Analysis and Machine Intelligence*, 5(2):206–213, March 1983.

[3] J. Jensen. Urban/suburban land use analysis. In J. Estes, editor, *Manual of Remote Sensing*, volume 2, pages 1571–1666. American Society of Photogrammetry, 1983.

[4] J. Lewis. Fast normalized cross-correlation. In *Vision Interface*, pages 120–123, 1995.

[5] R. Müller, T. Krauß, M. Lehner, G. Rönnbäck, and Å Karlsson. Image2006 GMES Fast track land service 2006–2008: Orthorectification of SPOT and IRS-P6 products. Technical report, DLR and Metria, May 2008.

[6] V. Nunes de Lima. *IMAGE2000 and CLC2000: Products and Methods*, volume EUR 21757 EN. European Commission, DG Joint Research Centre, 2005. URL `http://www.ec-gis.org/sdi/publist/pdfs/nunes2005eur2000.pdf`.

[7] P. Soille. IMAGE-2006 Mosaic: Cloud detection on SPOT-4 HRVIR, SPOT-5 HRG, and IRS-LISS III. Technical report, European Commission, DG Joint Research Centre, 2008.

[8] P. Soille and C. Bielski. IMAGE-2006 Mosaic: Data ingestion and organisation. Technical report, European Commission, DG Joint Research Centre, 2008.

[9] P. Soille and C. Bielski. IMAGE-2006 Mosaic: Product description. Technical report, European Commission, DG Joint Research Centre, 2008. In preparation.

[10] Q. Tian and M. Huhns. Algorithms for subpixel registration. *Computer Vision, Graphics, and Image Processing*, 35(2):220–233, 1986.

[11] C. Tucker, D. Grant, and J. Dykstra. NASA's Global orthorectified Landsat data set. *Photogrammetric Engineering and Remote Sensing*, 70(3):313–322, March 2004.

[12] D. Yuan and C. Elvidge. Comparison of relative radiometric normalization techniques. *ISPRS Journal of Photogrammetry and Remote Sensing*, 51(3): 117–126, June 1996. doi:`10.1016/0924-2716(96)00018-4`.

European Commission

EUR 23636 EN – Joint Research Centre – Institute for Environment and Sustainability
Title: IMAGE-2006 Mosaic: Geometric and Radiometric Consistency of Input Imagery
Author: Pierre Soille and Jacopo Grazzini
Luxembourg: Publications Office of the European Union
2011 – 27 pp. – 21.0 x 29.7 cm
EUR – Scientific and Technical Research series – ISSN 1831-9424 (online), 1018-5593 (print)
ISBN 978-92-79-20959-8
doi:10.2788/50967

Abstract
Within their domain of overlap, two images may differ in both geometry and radiometry. Consequently, when they are mosaiced, these differences may reveal the position of the seam lines even if they follow salient image structures such as roads and streams. A pair of overlapping images is said to be consistent if they are in agreement to one another in both geometry and radiometry. In this report, the consistency is measured using correlation computations and linear regressions. Measurements are produced for all existing pairs of overlapping images (given the 3,699 IMAGE-2006 input images, there are 29,447 such pairs). The quality layers of the IMAGE-2006 mosaics rely directly on these measurements. Indeed, the agreement between any pair of adjacent pieces of the mosaic is determined by the consistency measurements calculated within the domain of overlap of the two images leading to these two mosaic pieces.

The mission of the JRC is to provide customer-driven scientific and technical support for the conception, development, implementation and monitoring of EU policies. As a service of the European Commission, the JRC functions as a reference centre of science and technology for the Union. Close to the policy-making process, it serves the common interest of the Member States, while being independent of special interests, whether private or national.

JRC
EUROPEAN COMMISSION

LB-NE-23636-EN-N

ISBN 978-92-79-20959-8